

## Research Article

# Real-Time Optimization of Precast Concrete Component Transportation and Storage

Donghai Liu <sup>1,2</sup>, Xin Li <sup>1,2</sup>, Junjie Chen <sup>1,2</sup> and Rui Jin <sup>1,2</sup>

<sup>1</sup>State Key Laboratory of Hydraulic Engineering Simulation and Safety, Tianjin University, Tianjin 300350, China

<sup>2</sup>School of Civil Engineering, Tianjin University, Tianjin 300350, China

Correspondence should be addressed to Donghai Liu; liudh@tju.edu.cn

Received 18 November 2019; Accepted 30 January 2020; Published 19 March 2020

Academic Editor: Melina Bosco

Copyright © 2020 Donghai Liu et al. This is an open access article distributed under the Creative Commons Attribution License, which permits unrestricted use, distribution, and reproduction in any medium, provided the original work is properly cited.

The construction of prefabricated concrete structures involves many different types of precast concrete (PC) components. Improper arrangements of the transportation, storage, and hoisting of the PC components could lead to unnecessary relocation of PC components, causing a delay in construction progress. To address this problem, this paper presented a dynamic optimization method for PC component transportation and storage based on real-time scheduling and tracking. The real-time schedule can be extracted from a 4D building information model (BIM), and the position of PC components during the whole transportation process is tracked by a proposed tracking system which integrates the global navigation satellite system (GNSS) and the radio frequency identification (RFID) technology. A transportation optimization model was built to obtain a reasonable transportation plan based on real-time construction progress. A cyclic operation network (CYCLONE) simulation model for component storing and hoisting was proposed to calculate the on-site transportation time. A storage optimization model was proposed by considering the real-time transportation information to optimize the storage mode and storage position in the yard. The proposed models were solved in the context of a case study, which indicates that our method can reduce the on-site transportation time by 37% and effectively control the relocation times.

## 1. Introduction

Prefabricated concrete structure is recently gaining momentum in the architecture, engineering, and construction (AEC) industry. With this technique, a building product is constructed and delivered by assembling concrete components that have been precast in factories. Compared to traditional on-site concrete casting practice, the construction technique requires less on-site operation and labor resources and can yield higher construction quality within a shorter construction duration by causing less environmental pollution [1, 2]. However, the construction of prefabricated concrete structures is a relatively complex process that involves a series of operations such as component transportation, storage, hoisting, and installation. During the process, the PC component transportation and storage are critically important operations [3, 4], especially for the projects located in the

city center, where space available for PC component storage is limited. The transportation plan of PC components determines whether there would be sufficient components and space on-site, respectively, for construction and for storage [3]. The storage layout affects the time of hoisting, relocation times, and then the construction efficiency. Here, the word “relocation” refers to the operation of removing the above components in a stack of PC components, in order to access the desired component to be installed according to the construction sequence of PC components. This operation is typical in projects where PC components are randomly piled up in a storage site and can cause unnecessary waste of time spent on finding and relocating components. Not being able to scientifically arrange the transportation plan and storage layout will result in problems such as storing difficulties and relocation, leading to undesirable delays in the construction schedule [4, 5].

Despite the importance of transportation and storage of PC components, current industry practices are still confronted with many problems that hinder the PC component transportation and storage from being fully optimized. First, the transportation plan without considering the uncertainty of real-time progress of construction often brings difficulties in construction. When the as-built progress is ahead of the as-planned schedule or the delivery is delayed, it would lead to a shortage of available PC components on-site [3, 6]. When the as-built progress is behind the as-planned schedule, excessive PC components would arrive at the construction site before the storage yard has sufficient space, which causes difficulties in PC component storage on-site [2]. Second, in current practice, PC components arriving at the construction site are usually stacked randomly in the storage yard without considering the real-time construction schedule and the arrival of subsequent components [4]. As a result, the chances of relocation of PC components increase. Research efforts have been made in component transportation [7–10] and storage layout optimization [11–16]. However, few of the existing researches have attempted to address the problem of transportation planning under the real-time construction schedule and optimize PC component storage layout by considering the impact of random storage and the sequence of arriving components. The research gap calls for a critical need to address the optimization problem of PC component transportation and storage in a context of the dynamically changing construction schedule and component position. Not meeting the need will continue to allow the transportation and storage plan inconsistent with the actual construction progress to misguide the construction practice, leading to extensive delays and economic loss. In light of the above limitations, this paper proposed and solved several real-time optimization models for the transportation plan and storage layout of PC components based on real-time scheduling and material position tracking. Recent advancements in computer graphics and sensing provide useful tools for incorporating dynamic construction information into our study: 4D building information modeling (BIM) allows for the collection of real-time schedule information, while radio frequency identification (RFID) and global navigation satellite system (GNSS) allow for the tracking of PC components during the whole transportation process [17–22].

The contribution of this research is threefold. First, a dynamic optimization model for the transportation plan was proposed based on real-time construction progress. The model dynamically uses the actual PC component demands retrieved from an as-built 4D BIM as one of its constraints and thus can yield a transportation plan that is consistent with the actual construction progress. Second, a systematic framework for PC component tracking was developed, which integrates GNSS and RFID techniques to enable the positioning of components in both the indoor and outdoor environments. The framework allows for the whole-process tracking of PC components and can provide real-time component arrival information for the following storage optimization. Third, a dynamic storage optimization model was proposed to guide the placement of each PC component

by considering the real-time transportation tracking and construction schedule. The model can help reduce the relocation times and on-site transportation time and thus improve the construction efficiency.

## 2. Literature Review

*2.1. Review of Component Transportation.* Component transportation plays an important role in PC component construction. Not being able to deliver the PC components on time can bring difficulties to storage or construction progress [2, 7]. To avoid the difficulties, the transportation plan of PC components needs to be arranged reasonably. Some efforts have been made on transportation plan arrangement. Sometimes, conflict exists between precast concrete component factories and the contractor because the contractor prefers earlier delivery which forces the factories to compress their production process [8]. To resolve this conflict, Zhai et al. [8] proposed three models to optimize the transportation plan and achieve a balance between the factories and the contractor. The information inconsistency for different stakeholders is another problem for transportation plan arrangement. Xu et al. [7] proposed a cloud-based fleet management platform and share transportation information among the stakeholders through it, which helps to arrange the transportation plan more reasonably. Besides, Chang et al. [9] optimized the transportation plan aiming to maximize the transport vehicle utilization rate on the basis of analyzing the geometrical characteristics and installation sequence. In order to reduce the transportation cost as well as meet the requirements, Tang et al. [10] proposed a bilevel programming model to optimize the transportation plan.

*2.2. Real-Time Tracking Techniques for PC Components.* Many scholars have applied RFID technology for PC component or construction material tracking and information collection of the production supply chain and construction site [17–20, 23]. The BIM is a repository of architectural engineering that integrates the information (geometry, state, location, etc.) of a building in a 3D visualization manner. By combining the BIM with RFID technology, the superiority of visualizing and tracking PC components in a BIM was demonstrated [24]. A BIM platform-integrated RFID enabled the visibility and traceability of PC components in manufacturing, logistics, and on-site construction [21]. However, the transportation information in the platform is manually updated by the driver, and real-time transportation tracking is not realized. As a widely used positioning technology, the GNSS has been applied to PC component tracking. GPS technology was used to track the transportation process of PC components, based on which the time when the components will arrive at the construction site was predicted [25]. The RFID, GPS, and GMS technologies were also used comprehensively to collect the real-time location and other information of construction materials on-site [22, 26].

A 4D BIM combines the construction progress with a 3D BIM, which can dynamically simulate the construction

process and display the real-time construction progress. A model which integrated the BIM and capital path method (CPM) was proposed to guide the construction site layout at different stages of construction [27]. The 4D BIM was also applied on the ETO (engineering-to-order) prefabricated project to simulate the construction process and analyze the working time of each process [28]. The method was used to arrange the transportation plan of PC components, which helped improve the construction efficiency and reduce inventory, and also played a key role in the logistics management of materials. To provide an accurate design of the transportation order, quantity, and type of the PC component, a logistics planning and control model for PC components based on the construction simulation results obtained from the 4D BIM was proposed [29].

**2.3. Review of Component Storage Optimization.** The study of storage optimization for PC components was first carried out in the field of prefabricated factories [30, 31]. Based on the consideration of component size, storage method, and safety distance, the concept of storage zoning was proposed, and a component storage and transportation optimization model with the goal of minimizing storage cost and transportation cost was developed [30].

The storage of PC components is an important task for the layout design of the construction site. At present, extensive studies have been focused on the optimization of materials and equipment layout. By dividing the construction site into several segments with equal size to store materials or facilities in, the construction site layout was optimized using simulation and the genetic algorithm (GA) [11]. To yield the most appropriate size and location coordinates to store the equipment and materials on-site, the actual travel path was used to calculate the transportation distance on-site rather than the linear path in a BIM-based dynamic optimization model [12]. For a congested construction site where interior building spaces are also used for material storage, construction logistics optimization models were still established [13, 14]. Additionally, different construction stages of construction [15] and the uncertainty of transportation distance and frequency [16] were also considered in the optimization of the layout of the construction site.

**2.4. Limitations of Existing Researches.** Despite the advancements made by the above researches, existing studies on PC component transportation and storage still have the following limitations:

- (1) The existing researches on transportation plan arrangement overlook the influence of uncertainty of the construction schedule. The difference between the real-time progress and the designed schedule should be considered.
- (2) Transportation tracking information is not taken into account in the existing researches, leading to an overlook of the impact of upcoming components on storage optimization.

- (3) Few efforts have been made to optimize the storage of PC components in the construction site. The impact of random storage and repeated relocation on construction efficiency has not been considered. In addition, different types of PC components are simplified as one kind of material [12], which is not accurate enough to decide the location to store and hoist each type of component.

### 3. Methodologies

In order to address the limitations of existing researches, this paper proposed two real-time optimization models for the transportation plan and storage layout, respectively, and a CYCLONE simulation model of storing and hoisting. As shown in Figure 1, the models are based on the information retrieved from a 4D BIM and a real-time tracking system of PC components. The 4D BIM is used to obtain the real-time demand of PC components. The real-time tracking system integrated with RFID and GNSS is used to obtain the location of PC components, through which the arriving time, type, and quantity of components can be predicted. The transportation optimization model is solved by a linear programming solver, while the storage layout optimization model is solved by CYCLONE simulation and genetic algorithms.

**3.1. Transportation Optimization Based on Actual Demands.** A model is proposed to optimize the transportation plan of PC components by considering the real-time construction progress and demand. A 4D BIM integrates the construction schedule with the BIM, from which the real-time construction progress can be obtained and the actual demand of components under the current progress can be further analyzed, to assist the formulation of the transportation plan.

**3.1.1. Objectives.** The model assumes that a prefabricated project requires  $I$  different types of PC components supplied by  $J$  different factories. The on-site staff releases transportation orders of PC components to the factories according to the current construction schedule and a reasonable estimation. The required PC components will then be delivered to the construction site within  $T$  days after the order is released. The variable for the proposed model can be expressed as  $X(i, j, t)$ , which stands for the quantity of type  $i$  components arriving at the site on the  $t$ th day from the  $j$ th factory ( $t = 1, 2, \dots, T, j = 1, 2, \dots, J, i = 1, 2, \dots, I$ , and  $X(i, j, t)$  is an integer). The model has the following two optimization objectives:

- (1) Minimizing the transportation cost  $Z_1$ : the model assumes that the same type of vehicle is used to transport the PC components, and the transportation cost of unit distance is fixed. The transportation cost is calculated by the following equation:

$$\min Z_1 = \sum_{j=1}^J \sum_{t=1}^T b(j, t) \cdot d(j), \quad (1)$$

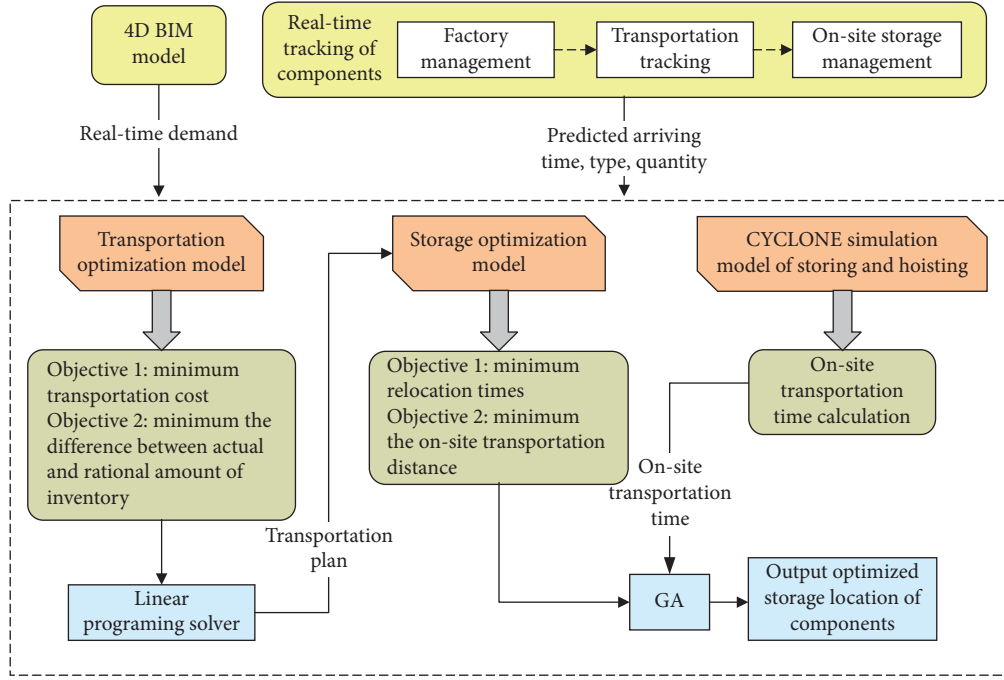


FIGURE 1: Overall research methodology.

where  $b(j, t)$  is the number of transport vehicles sent from the  $j$ th factory on the  $t$ th day and  $d(j)$  is the distance from the  $j$ th factory to the construction site.

- (2) Minimizing the difference between the actual amount and the rational amount of the PC component inventory on-site  $Z_2$ : although the model is based on real-time progress, there still exist uncertainties in the subsequent construction. Increasing the component inventory on-site can meet the needs when the construction speed exceeds the expected speed. However, once the construction speed is lower than the expected speed, there may be no space on-site to store the excessive components. Considering the uncertainty of the demand and schedule, the on-site inventory buffer coefficient  $u$  is introduced to determine a rational amount of the PC component inventory, which is  $u$  times the demand. The objective is to minimize the difference between the inventory amount and this rational amount, as follows:

$$\min Z_2 = \sum_{t=1}^T \sum_{i=1}^I |Q(i, t) - u \cdot D(i, t + 1)|, \quad (2)$$

where  $Q(i, t)$  is the inventory amount of the  $i$ th component on the  $t$ th day and  $D(i, t + 1)$  is the demand of the  $i$ th component on the  $t + 1$ th day.

### 3.1.2. Constrains

- (1) *Production Capacity Constraints.* The quantity of PC components which are available in each factory each day is limited, so the transportation plan is subject to the production capacity of the factories, as shown by

$$X(i, j, t) \leq C(i, j), \quad (3)$$

where  $C(i, j)$  is the quantity of the  $i$ th type of component that the  $j$  component factory is able to provide.

- (2) *Demand Constraints.* In order to meet the construction demand, the number of components stored on-site should be no less than the demand for the next day, as shown by the following equations:

$$Q(i, t) \geq D(i, t + 1), \quad (4)$$

$$Q(i, t) = Q_0(i) + \sum_{n=1}^t \sum_{j=1}^J X(i, j, n) - \sum_{n=1}^t D(i, n), \quad (5)$$

where  $Q_0(i)$  is the initial stocking amount of the  $i$ th component.

- (3) *Storage Yard Area Constraints.* The transportation plan should be formulated within the scope of on-site storage yard capacity, as illustrated by the following equation:

$$\sum_{i=1}^I \frac{Q(i, t)}{A(i)} \leq 1, \quad (6)$$

where  $A(i)$  is the maximum quantity of the  $i$ th component allowed to be stored in the storage yard and  $Q(i, t)/A(i)$  represents the percentage of the storage yard area that the  $i$ th component is occupying.

*3.1.3. Model Solving.* The model proposed above is a multiobjective integer linear programming model with  $T \times I \times J$  integer variables and is solved by a linear programming



solver. The linear weighting method is used to construct the evaluation function. Normalization has been performed to ensure the consistency of dimensions of the two objectives, as is shown by the following equation:

$$f = a \cdot \frac{Z_1 - \min Z_1}{\max Z_1 - \min Z_1} + b \cdot \frac{Z_2 - \min Z_2}{\max Z_2 - \min Z_2}, \quad (7)$$

where  $a$  and  $b$  are the weights of the two objectives, respectively, and  $a + b = 1$ ;  $\min Z_m$  and  $\max Z_m$  ( $m = 1, 2$ ), respectively, represent the minimum and maximum values of the single objective model under the same constraints.

Gurobi solver is used to solve the model. As a large-scale mathematical programming solver, the Gurobi solver can provide quick and precise solutions for multivariable and multiconstraint optimization models, such as integer programming, linear programming, and quadratic programming. A MATLAB interface provided by the Gurobi solver was used to derive the solutions of the model.

**3.2. Whole-Process Tracking of PC Components.** A systematic framework is developed to enable the whole-process tracking of PC components, which is mainly composed of three parts, i.e., component factory management, transportation tracking, and on-site storage management.

**3.2.1. Factory Management.** RFID registration techniques are used in the stage of factory management. Before PC components are transported out of the factory, an RFID tag is embedded in each component. The embedded tag is scanned by a handheld RFID reader to upload the information, such as the PC component ID, type, manufacturer, and current state, to the system. On being loaded onto transport vehicles, the PC components need to be scanned again to bind the components with the transport vehicles. In the meantime, the state of the PC components in the system database is changed on the handheld reader. The process is shown in Figure 2(a).

**3.2.2. Transportation Tracking.** The transport vehicles are equipped GNSS-positioning devices to provide real-time geographical information of the vehicles. Since each vehicle has been associated with the PC components it carries at the factory management stage, the transportation route and the geographic position information of the PC components can also be obtained in real time. With the position information and an estimation of transportation speed, the arriving time of the PC components can be predicted to guide the planning of the storage layout in advance. Figure 2(b) shows an example of the transportation route and the position of a vehicle.

**3.2.3. On-Site Storage Management.** On arrival, the RFID tags embedded in the PC components are scanned to update the location information of the components to the system. According to the storage location determined by the storage optimization model, the PC components are placed into the

storage yard. During construction, the component is hoisted from the location which is determined by the simulation model. A BIM of the storage yard is created and dynamically updated to reflect the actual PC component layout, as is shown in Figure 2(c).

### 3.3. Establishment of Dynamic Storage Optimization Model

**3.3.1. Premises and Assumptions.** The proposed model is based on the following premises and assumptions:

- (1) The real-time schedule obtained from the 4D BIM and transportation tracking information is readily available so that the arrival time, type, and quantity of in-transit components in a certain time period ( $T$  days) can be predicted.
- (2) The time period ( $T$  days) of the storage optimization model is set equal to that of the transportation optimization model proposed above to ensure that the transportation plan and tracking information are available.
- (3)  $T$  is divided into  $K$  shorter time periods with the equal interval  $A$ , on which the simulation of component storing and hoisting is based. At the beginning of each shorter time period, the components that have arrived during the previous shorter period are uniformly stacked. The proposed model only aims to optimize the storage position of PC components at the beginning of the first shorter period of  $T$  days to ensure that the newest schedule and transportation tracking information are used. Besides, component storing and hoisting in a certain time period ( $T$  days) are considered in the storage optimization model to analyze the impact of component storage in the first period on subsequent construction and components' storage.
- (4) In order to ensure that the quantity of PC component storage on-site at least satisfies the construction demand in one day, the model assumes that the components demanded in one day have been already stored on-site.
- (5) According to the storage mode, all the PC components can be divided into four categories, i.e., vertical storage components (wallboard, etc.), tiled storage components (composite beam, etc.), same-type stacking components (stairs, etc.), and mixed-type stacking components (laminated slab, etc.).
- (6) Referring to [11, 30], this paper divides a storage yard into  $E$  equal-sized storage zones. Only components of the same storage mode can be stacked in the same storage zone before the storage zone is empty again, and the number of storage zones is determined by the site manager. Each storage zone is further divided into several bays, where a piece or a pile of components is stored. Because the components of the same storage mode tend to have similar sizes, the quantity of bays in each zone is determined

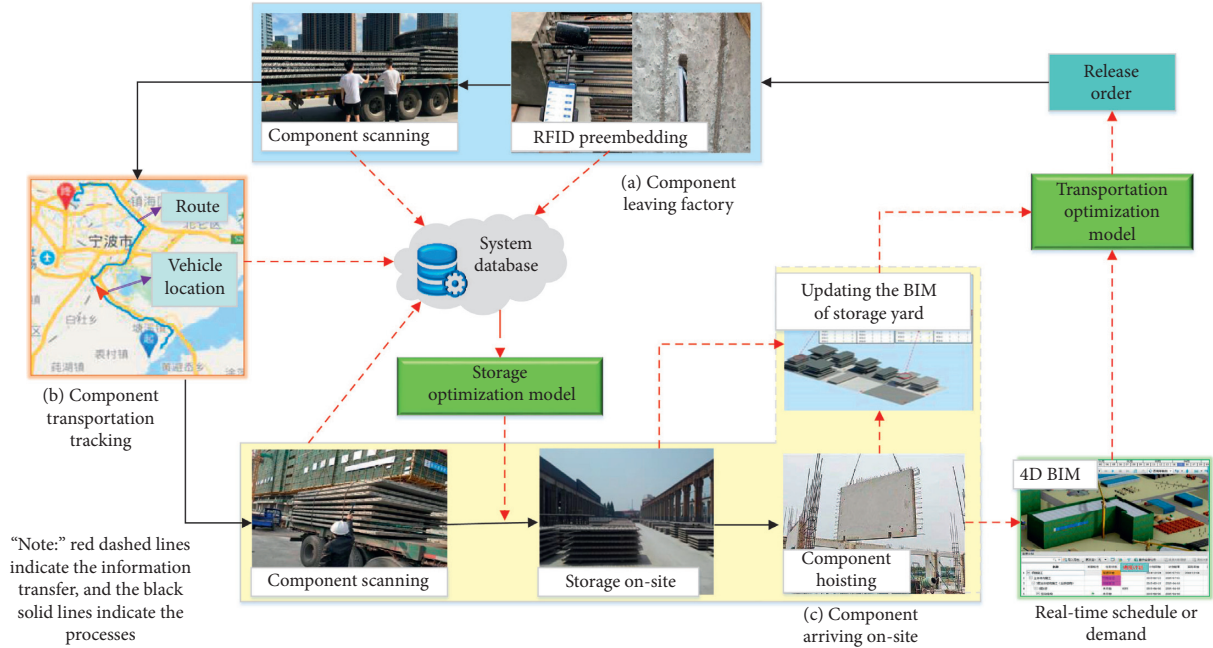


FIGURE 2: Schematic diagram of whole-process transportation tracking.

according to the storage mode in the storage zone. Figure 3 shows a schematic diagram of a storage yard ( $E=6$ ), where  $e$  and  $m$  represent the storage zone number and the bay number, respectively.

**3.3.2. Optimization Variables.** The variable  $X$  of the storage optimization model is set as the state (type and quantity of components) of each bay in each storage zone of the storage yard. In this way, the size of variables is determined by the storage yard only and easy to control, which can help improve the solving efficiency. The state of the yard is updated every time the component storage is completed in a shorter time period. Therefore, the variable  $X$  consisted of  $K$  storage states, and each state  $X_k$  represents the storage state of period  $k$  after storage,  $k = 1, 2, \dots, K$ .

The storage state at the end of each period consists of the states of each bay. A column vector is used to represent the storage state of a bay. The column vector can be divided into two parts, as shown in Figure 4. The first part is the first element of the vector, which indicates the component storage mode of the bay—0 for no component stored, 1 for the vertical storage, 2 for the tiled storage, 3 for the same-type stacking, and 4 for the mixed-type stacking. The remaining elements make up the second part, which indicate the type and quantity of components. The column vector length  $U$  is determined by the maximum allowable amount of the mixed-type storage components  $h_{\max}$ ,  $U = h_{\max} + 1$ , which will be explained below.

When the storage mode of a zone is vertical storage, tiled storage, or same-type storage, the stacking order in a bay of the zone is not considered. Note that each bay can only contain a vertical storage component or a tiled storage component. Hence, for the above three storage modes, only the first three elements of the column vector are needed,

which represent the storage condition of the bay, the component type, and the quantity, respectively. The remaining elements are set as 0. An example of such vectors is shown in Figure 4(a). When the storage mode of the zone is mixed-type stacking, the second to the last elements, respectively, indicate the type of the components stored in the bay from top to bottom. As shown in Figure 4(b), 4 components are piled up in the bay, and the types of them from the top layer to the bottom layer are  $i_2, i_3, i_4$ , and  $i_4$ , respectively. By combining the column vectors of all the  $M$  bays in  $E$  zones at all the  $K$  shorter periods, the storage state variable, which is a matrix of size  $U \times (KEM)$ , can be obtained, and  $M$  is determined by the largest number of bays among the  $E$  storage zones.

### 3.3.3. Objectives

- (1) Minimizing the weighted transportation distance  $P$  in the construction site: the transportation distance is represented by the linear distance from the center point of the storage zone to the tower crane. Considering that components with larger size are more difficult to transport than smaller ones, the transportation difficulty coefficient  $w_i$  is introduced to indicate the transportation difficulty of the type  $i$  component. The objective function is formulated as

$$\min P = \sum_{k=1}^{K+1} \sum_{i=1}^I \sum_{e=1}^E y_{i,k,e} \cdot d_e \cdot w_i, \quad (8)$$

where  $y_{i,k,e}$  is the quantity of type  $i$  components hoisted from the storage zone  $e$ , during period  $k$ , and  $d_e$  is the linear distance from the storage zone  $e$  to the tower crane.

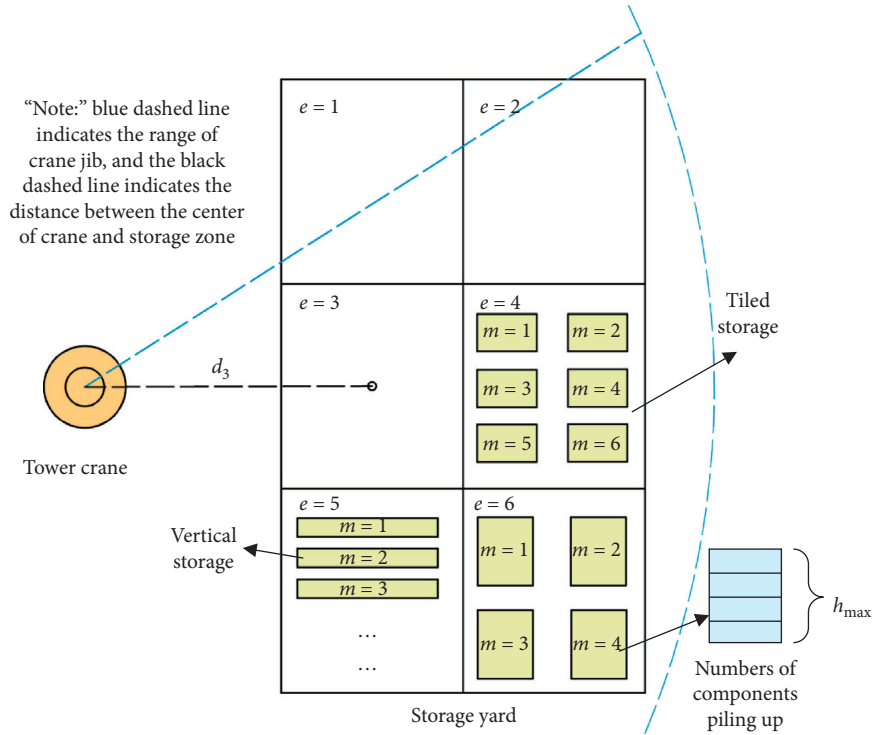


FIGURE 3: Schematic diagram of the storage yard.

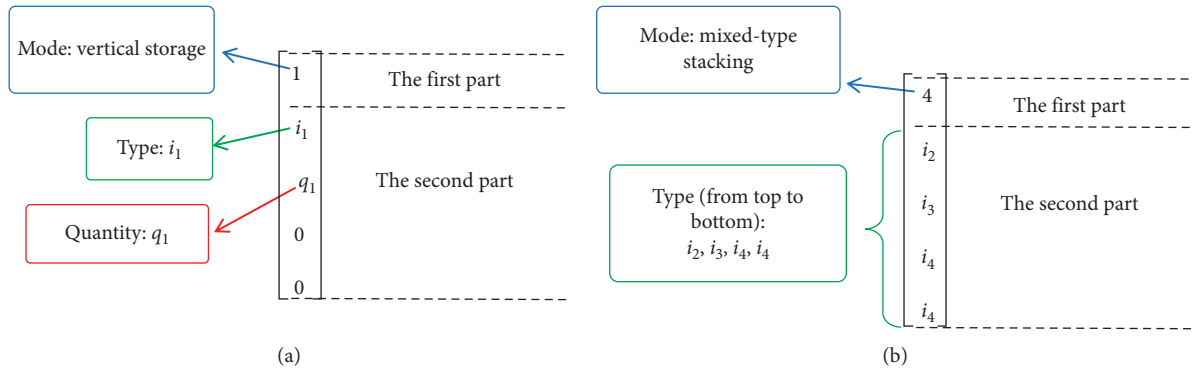


FIGURE 4: Vectors used to describe the bay storage state of different storage modes: (a) vertical, tiled, and same-type stacking; (b) mixed-type stacking.

(2) Minimizing relocation times  $R$ : the objective function is formulated as the following equation:

$$\min R = \sum_{k=1}^{K+1} \sum_{i=1}^I r_{i,k}, \quad (9)$$

where  $r_{i,k}$  is the number of relocation times when the type  $i$  component is hoisted in period  $k$ .

$$\begin{cases} \sum_{m=1}^M \frac{X(1, J+m)}{z} \leq A_z, & z = 3, 4, \\ \sum_{m=1}^M X(3, J+m) \leq A_z, & z = 1, 2, \\ J = (k-1) \times M \times E + (e-1) \times M, \end{cases} \quad (10)$$

### 3.3.4. Constraints

(1) *Space Constraints.* The number of bays must not exceed the maximum number of bays allowed in a storage zone, as illustrated by

where  $z$  is the storage mode of a bay;  $A_z$  is the maximum allowed number of bays under the current storage mode;  $k = 1, 2, \dots, K$ ;  $e = 1, 2, \dots, E$ ; and  $m = 1, 2, \dots, M$ .

(2) *Stacking Height Constraints.* For components that can be piled up, the number of layers must not

exceed the maximum number allowed by safety considerations:

$$\begin{cases} X(3, J+m) \leq H_3^{\max}, & X(1, J+m) = 3, \\ \sum_{u=2}^U \frac{X(u, J+m)}{X(u, J+m)} \leq H_4^{\max}, & X(1, J+m) = 4, \\ J = (k-1) \cdot E \cdot M + (e-1) \cdot M, & k = 1, 2, \dots, K, e = 1, 2, \dots, E, \end{cases} \quad (11)$$

where  $H_3^{\max}$  and  $H_4^{\max}$  are the maximum allowable number of piled-up layers of the same-type stacking components and the mixed-type stacking components, respectively, and  $m = 1, 2, \dots, M$ .

(3) *Total Amount Constraint.* The constraint of the total component amount can be formulated as

$$Q_{k,i} = Q_{k,0} - \sum_{j=1}^{k-1} D_{i,j} + \sum_{j=1}^k q_{i,j}, \quad (12)$$

where  $Q_{k,i}$  is the quantity of the components of type  $i$  at the end of period  $k$ ;  $D_{i,k}$  represents the demand of the component of type  $i$  during the  $k$  period; and  $q_{i,k}$  is the components of type  $i$  stored in period  $k$ ;  $k = 1, 2, \dots, K$ .

(4) *Logical Constraints.* The model should also meet the following two logical constraints: First, if the storage condition of the bay is empty, all variables of the column vector representing this bay are set as 0. Second, when the storage mode of a zone is vertical storage, tiled storage, or same-type storage, only the first 3 rows of the column vector are occupied with the storage mode, the component type, and the quantity and the elements of the remaining rows must be 0.

**3.4. GA-Simulation-Based Solution for the Storage Optimization Model.** The proposed storage optimization model is a multiobjective integer programming model with  $U \times (KEM)$  integer variables and is solved by a simulation-based genetic algorithm (GA). The flowchart of the solving process is shown in Figure 5. The genetic algorithm is used to generate variables that satisfy the constraints. The generated variables and parameters are then input to the simulation model of the component storing and hoisting process for transportation time calculation. The GA optimization operation persists until the fitness value of the results in certain generation meets the terminating condition. After getting the optimized storage state by the GA-simulation method, the specific storage location of each component is to be calculated by the difference between the optimized state and the state just before the storage happens, which is obtained from the

simulation model. The storage location of each PC component is output as a result of the model at the end.

**3.4.1. CYCLONE Simulation Model for PC Component Storing and Hoisting.** In order to calculate the on-site transportation time, the process of the PC component storing and hoisting is simulated. CYCLONE has been applied in construction simulation of dams, underground powerhouses, tunnels [32, 33], etc. In this paper, the CYCLONE simulation technology is adopted, as shown in Figure 6. The simulation runs on a period basis. After the components are hoisted for  $N$  times in period  $k$ , the components arriving during the period are uniformly stacked at the end of the period. Thus, the functional node is set in the simulation model. The number of cycles  $N$  is the number of components being hoisted during the period, which is determined by the average construction speed. Since the storage of PC components does not occupy the tower crane and has no effect on the construction progress, the time for component storage is ignored in calculating the transportation time on-site.

The calculation process of on-site transportation time is shown in Figure 7. The data input at the beginning of the simulation is as follows: the initial state of the storage yard, the hoisting order  $I_k$  ( $k = 1, 2, \dots, K$ ), the total quantity of components to be hoisted  $N_{\text{sum}}$ , the quantity of components in each period  $N_k$  ( $k = 1, 2, \dots, K$ ), the time cost for each relocation, the time to connect a component and the crane, the vertical and horizontal speed of the tower crane, the distance between storage zones and the tower crane, the number of optimization periods  $K$ , and the state of the storage yard  $X$ .

The same type of components can be stored in different places in the storage yard. Hence when a component is needed, the place from where the component is hoisted should be decided. Two principles are generally used to determine the place, i.e., minimizing relocation times and minimizing distance. These two principles might conflict with each other sometimes. To compare the influence of the two principles on the construction speed, two simulation rules are proposed: one considers the distance first and the other considers relocation times first. The on-site transportation time  $t(n)$  of a component can be calculated as follows:



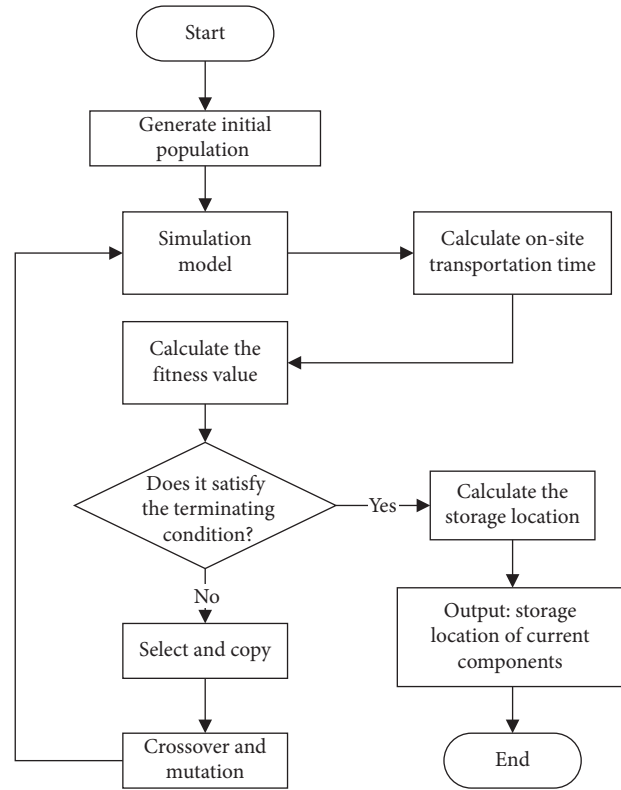


FIGURE 5: Flowchart of the solving process of the storage optimization model.

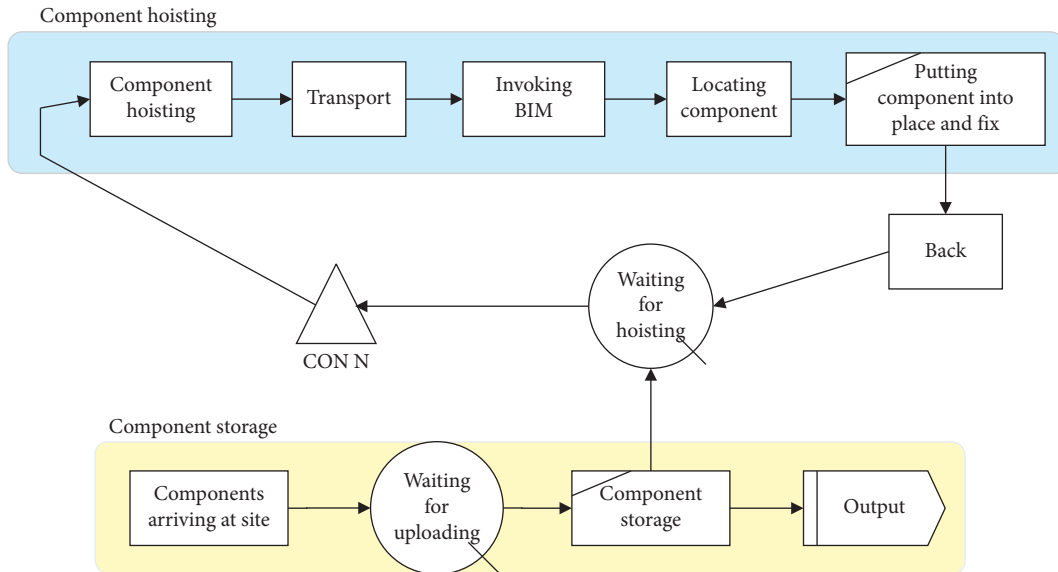


FIGURE 6: CYCLONE simulation model for component storing and hoisting.

$$t(n) = (t_d + t_v + t_h + t_f) \cdot w_i, \quad (13)$$

where  $t_d$  is the time to connect the unit component and crane;  $t_v = 2d_e/v_v$  is the component horizontal transportation time, in which  $v_v$  is the horizontal transportation speed of the crane;  $t_h = h/v_h$  is the vertical transportation time, in which  $h$  is the vertical transportation height and  $v_h$  is the lifting speed of the crane;  $t = c \cdot a$  is the relocation time, in which  $c$  is the time

cost per relocation and  $a$  is the number of relocations; and  $w_i$  is the transportation difficulty coefficient.

### 3.4.2. Genetic Algorithm for Solving Storage Optimization Model

(1) *Fitness Function.* The proposed storage optimization model is a multiobjective optimization model, which is

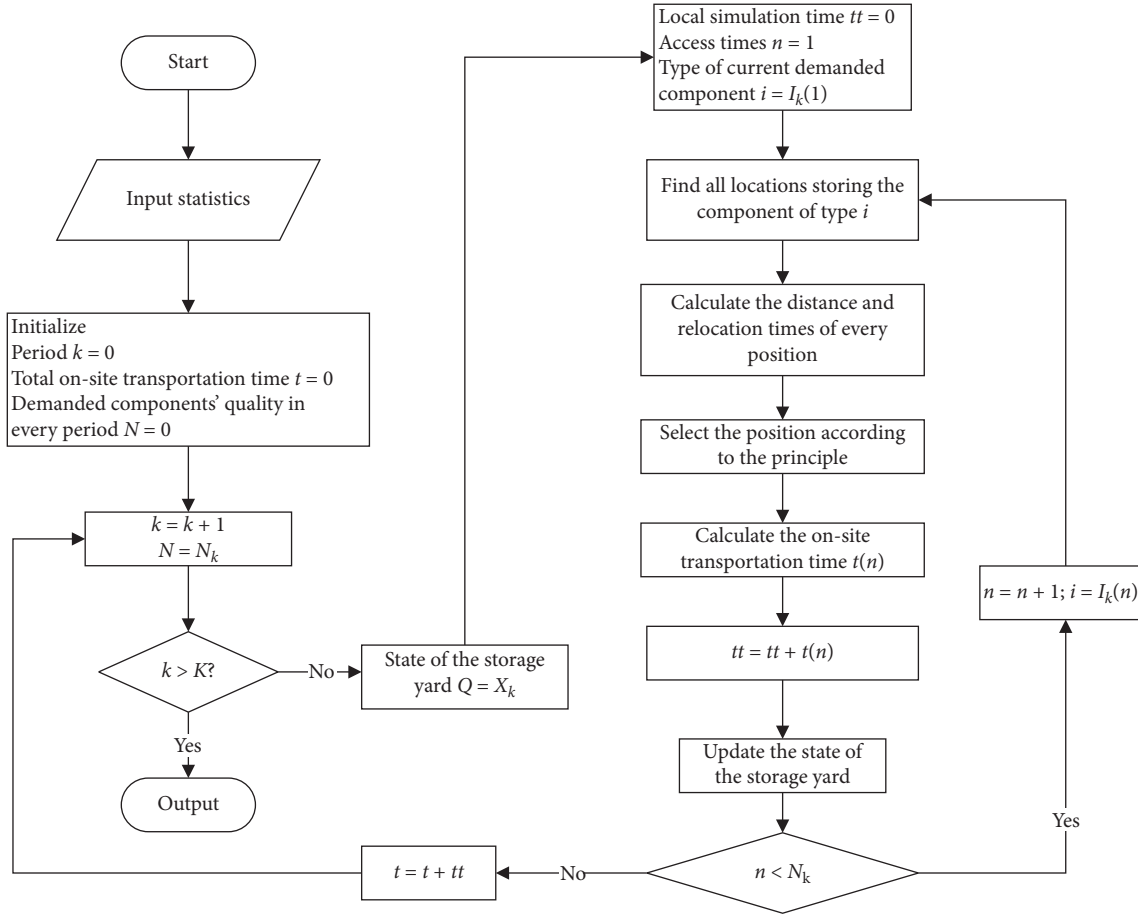


FIGURE 7: Flowchart for calculating on-site transportation time using simulation.

normally solved by a weighted evaluation function. However, the model's objectives have different dimensions which are difficult to normalize. Moreover, the relocation times and transportation distance both affect the construction speed by affecting the on-site transportation time of the PC components. Therefore, the on-site transportation time obtained by the simulation model can reflect the fitness value of the solution. Besides, the equality constraint (total amount constraint) is difficult to satisfy in generating the initial population and the genetic operation, so a penalty function is used to reflect whether the equality constraint is satisfied. The fitness function is as follows:

$$\begin{cases} f = \frac{1}{T_T \cdot y_p}, \\ y_p = (M \cdot n_p)^2, \end{cases} \quad (14)$$

$$n_p = \sum_{k=1}^K \sum_{i=1}^I Q_{k,i} - \left( Q_{k,0} - \sum_{j=1}^{k-1} D_{i,j} + \sum_{j=1}^k q_{i,j} \right),$$

where  $T_T$  is the on-site transportation time obtained by simulation;  $M$  is the penalty coefficient; and  $n_p$  is the deviation between the two sides of the equality constraint.

(2) *Coding Method.* The variable of the model is a matrix, which cannot be simply and directly represented by a conventional one-bit coding method (binary coding, real coding, etc.). Therefore, the matrix coding is used to represent the variable, as shown in Figure 8.

(3) *Initial Population.* The initial population of the model is difficult to generate with a traditional random method for its large dimensions and complicated constraints. Therefore, the following two principles are proposed to guide the generation of initial population: First, only after one storage zone is fully filled, the next storage zone can be used to store components of the same storage mode. Second, the generated initial population and genetic operation should meet the area constraint, the height constraint, and the logical constraint, and the quantity constraint is included as a penalty function.

(4) *Genetic Operation.* The algorithm adopts the roulette selection strategy, and the probability of being selected as parents increases with the fitness value. An elitism strategy is used to ensure that good genes can be inherited to offsprings. The offspring population is generated through the following genetic operations:

(i) *Adaptive crossover operator:* it dynamically changes the crossover rate based on the fitness value of the parents. Individuals with higher fitness

$$X_k^i = \begin{bmatrix} g_{11}^i & g_{12}^i & \cdots & g_{1n}^i & g_{1(an+1)}^i & g_{1(an+2)}^i & \cdots & g_{1(an+n)}^i \\ g_{21}^i & g_{22}^i & \cdots & g_{2n}^i & g_{2(an+1)}^i & g_{2(an+2)}^i & \cdots & g_{2(an+n)}^i \\ \vdots & \vdots & & \vdots & \vdots & \vdots & & \vdots \\ g_{m1}^i & g_{m2}^i & & g_{m2n}^i & g_{m(an+1)}^i & g_{m(an+2)}^i & \cdots & g_{m(an+n)}^i \end{bmatrix}$$

State of storage yard after storage in period 1
State of storage yard after storage in period a

FIGURE 8: Dimensions of the matrix variable of the model.

values than an average value will have a lower crossover rate to allow their good genes to be kept in offspring population. On the contrary, individuals with a lower fitness rate will have higher crossover rates. The operator can ensure the diversity of the population and prevent it from falling into a local optimum. The formula for calculating the crossover rate is shown as

$$P_c = \begin{cases} \frac{k_1(f_{\max} - f)}{f_{\max} - f_{\text{avg}}}, & f \geq f_{\text{avg}}, \\ k_2, & f < f_{\text{avg}}, \end{cases} \quad (15)$$

where  $P_c$  is the crossover rate;  $f_{\max}$  is the maximum fitness value of the population;  $f_{\text{avg}}$  is the average fitness value of the population;  $f$  is the larger fitness value of the two individuals to be crossed; and  $k_1$  and  $k_2$  are parameters and  $k_1 < k_2$ . The single-point crossover is used as the crossover mode, and the crossover node  $n$  is generated randomly. The node  $n$  represents period  $n$  in the storage model. As shown in Figure 9(a), the storage state from period 1 to period  $n$  of the parent  $i$  is combined with the storage states from period  $n + 1$  to period  $N$  (the last period) of the parent  $j$  to constitute a new offspring individual.

- (ii) Mutation operator: the mutation node  $n$  is randomly generated. The variables before the node are reserved and the variables after the node are regenerated, which means that the storage state after the  $n$ th period is reestablished, as shown in Figure 9(b).
- (iii) In order to prevent the solution falling into a local optimum, some of the offspring individuals will be regenerated to introduce new genes into the population when the optimal solution does not change within the certain number of iterations.

## 4. Case Study

**4.1. Project Background.** The D project is located in Z Province, China. It consists of 13 townhouses, 9-storey bungalows, and 4 high-rise buildings with a total construction area of 100595.6 m<sup>2</sup>. The structure type is the frame

shear wall structure combined with PC prefabrication. PC composite beams, PC composite slabs, PC stairs, and other PC components are used in the project. RFID and BeiDou (Chinese Global Navigation Satellite System) positioning systems are used to track PC components in real time.

The project uses the 4D BIM to reflect the construction progress and to carry out dynamic project management. Figure 10 shows interfaces of the 4D BIM. The component quantity demanded in next two days is calculated through the BIM based on the current progress, and a list of PC component requirements is shown in the table at the bottom right of Figure 10. In order to implement real-time tracking and visualization of PC components on the yard, the storage yard is also separately modeled. The storage yard BIM is modeled based on the information obtained from the whole-process tracking system of PC components and displays the state of the storage yard in real time. Connecting the storage yard BIM with RFID technology supports to realize the whole-process management of PC components on-site.

**4.2. Model Establishment and Solution.** The construction of building #21 in the project was taken as an example. The transportation plan was released each two days in the project. Consequently, the optimization period  $T$  of both the transportation optimization model and the storage optimization model was set as 2 days. According to the current progress, the construction of a standard floor should be completed in the period, and a total of 68 PC composite slabs of 42 types are going to be used in the construction. Assuming that the construction speed was uniformly distributed, 34 components would be constructed per day. Table 1 shows the demand and supply of the PC components. The “De.” and “Seq.” columns show the demand and construction sequence of each type of component in the optimization period (2 days), respectively. The “Fac.” column shows the code number of the factory that is able to supply the components, and the corresponding quantity that can be supplied per day by the factories is shown in the “Supply per day” column. The quantity of PC components initially stored in the storage yard was exactly equal to the quantity demanded on the first day. The storage yard had a size of 10 × 21 m<sup>2</sup>, which was divided into six 5 × 7 m<sup>2</sup> storage zones. The horizontal linear distance from each storage zone to the tower crane was 15.3 m, 16.9 m, 19.3 m, 20.5 m, 23.3 m, and 24.3 m, respectively. The distance between each two bays in a storage zone was at least 1 m. The PC composite slabs were stored in the mixed-type storage mode, and two storage bays were set in each storage zone considering the maximum size of components. The components cannot pile up with more than 6 layers in a bay for the safety consideration.

**4.2.1. Solution of Transportation Optimization Model.** Three factories, i.e., factories I, II, and III, supplied PC components for the project, which were 200 km, 160 km, and 300 km away from the construction site, respectively. The

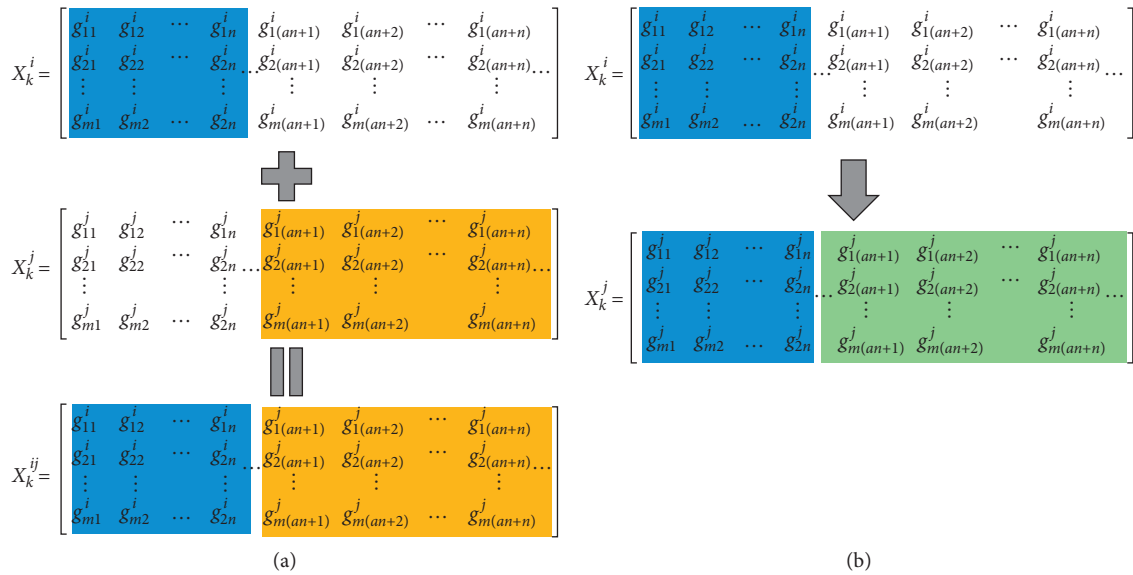


FIGURE 9: Genetic operators: (a) crossover operator; (b) mutation operator.

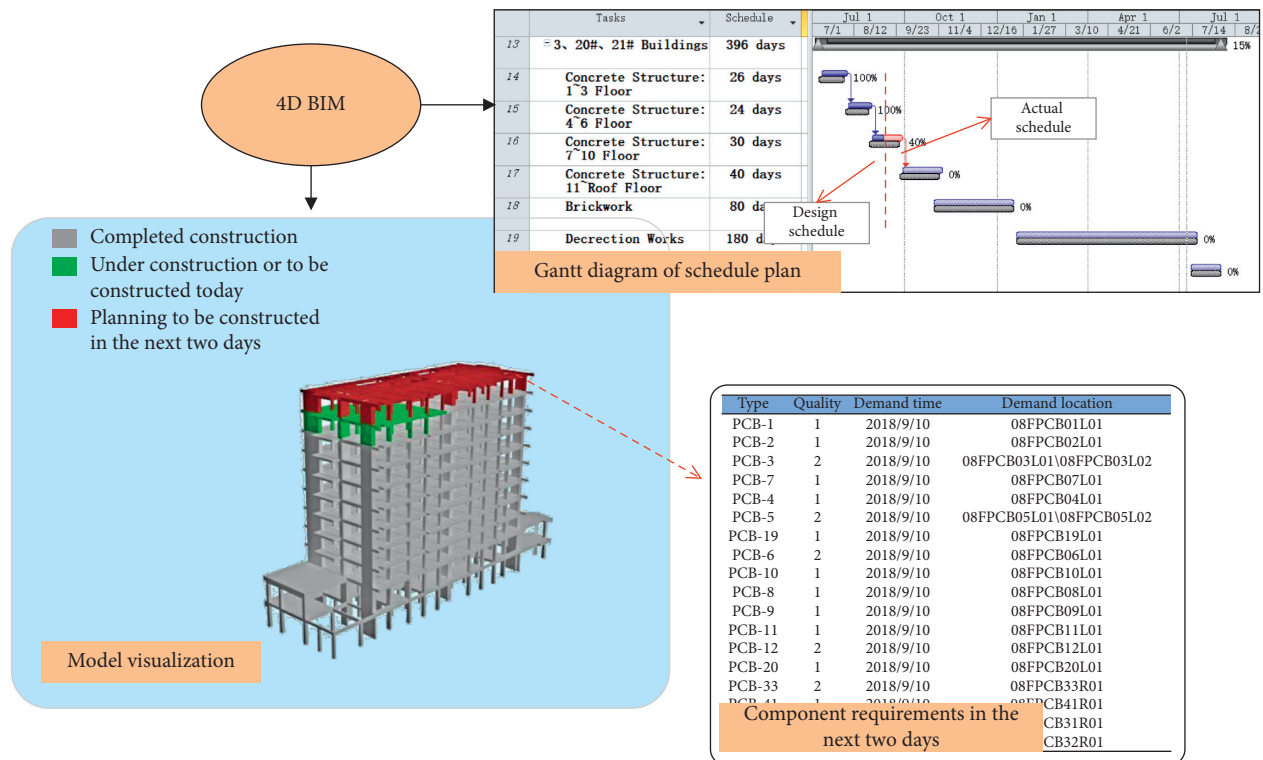


FIGURE 10: 4D BIM of the demonstration project.

types of components produced by each factory and the constraints of supply per day are shown in Table 1. PC components were transported using 10-meter long flatbed trailers, and each trailer can be loaded with 12 PC components.

According to the site situation, the value of the on-site inventory buffer coefficient  $k$  was set as 1.5 [25]. The weights

of the two objectives (i.e., minimum transportation cost and minimum difference between actual and rational amount of the inventory) were set as 0.6 and 0.4, respectively. The transportation optimization model was solved by the Gurobi solver, and the optimal fitness value is 0.0949. The optimized transportation plan for two days is shown in Table 2, and the component quantity of each type is shown in the brackets.



TABLE 1: Demand and supply of PC components for the construction of a standard floor.

Type	De.	Seq.	Fac.	Supply per day
pcb-1	1	1	I, III	2, 2
pcb-2	1	2	I, III	2, 2
pcb-3	2	3, 6	I, III	2, 2
pcb-4	1	5	I, III	2, 2
pcb-5	2	7, 8	I, III	2, 2
pcb-6	2	10, 11	I, III	2, 2
pcb-7	1	4	I, III	2, 2
pcb-8	2	13, 45	I, II	2, 2
pcb-9	2	14, 46	I, II	2, 2
pcb-10	2	12, 44	I, II	2, 2
pcb-11	2	15, 47	I, II	2, 2
pcb-12	4	16, 17 48, 49	I, II	2, 2
pcb-13	1	28	I, II	2, 2
pcb-14	1	29	I, II	2, 2
pcb-15	2	30, 32	II, III	2, 2
pcb-16	1	31	II, III	2, 2
pcb-17	1	26	II, III	2, 2
pcb-18	2	33, 34	II, III	2, 2
pcb-19	1	9	II, III	2, 2
pcb-20	2	18, 50	II, III	2, 2
pcb-21	1	27	II, III	2, 2
pcb-22	1	60	I, III	2, 2
pcb-23	1	61	I, III	2, 2
pcb-24	2	62, 65	I, III	2, 2
pcb-25	1	64	I, III	2, 2
pcb-26	2	66, 67	I, III	2, 2
pcb-27	2	58, 59	I, III	2, 2
pcb-28	1	63	I, III	2, 2
pcb-29	2	24, 56	I, II	2, 2
pcb-30	2	25, 57	I, II	2, 2
pcb-31	2	22, 54	I, II	2, 2
pcb-32	2	23, 55	I, II	2, 2
pcb-33	4	19, 20 51, 52	I, II	2, 2
pcb-34	1	42	I, II	2, 2
pcb-35	1	43	I, II	2, 2
pcb-36	2	35, 37	II, III	2, 2
pcb-37	1	36	II, III	2, 2
pcb-38	1	40	II, III	2, 2
pcb-39	2	38, 39	II, III	2, 2
pcb-40	1	68	II, III	2, 2
pcb-41	2	21, 53	II, III	2, 2
pcb-42	1	41	II, III	2, 2

4.2.2. *Solution of Storage Optimization Model.* The optimization period was two days, and the working hours of each day was 8 hours. Therefore, the optimization time period  $T$  was 16 hours. The PC components were stored each 2 hours ( $A = 2$ ), and the number of periods  $K = T/A = 8$ . The number of storage zones  $E$  equaled 6, and the number of bays in each storage zone  $M$  equaled 2. Hence, the size of the matrix variable was  $7 \times 96$ . In this case study, the optimization model was used to obtain the storage location of components arriving during the first one of the 8 periods. Therefore, the model was solved according to the real-time transportation tracking information at the beginning of the first period. At this point, the expected delivery time and the sequence of the PC components in the next 8 time periods can be predicted, as shown in Table 3.

(1) *Results of the GA-Simulated Solution.* The maximum weight of the PC components in this project was 1.7 t, and the nominal speed of the tower crane was constant when the hoisted components are less than 3 t. Therefore, the transportation difficulty coefficient  $w_i$  of each component is 1. The nominal lifting speed of the tower crane is 40 m/min, the horizontal speed is 20 m/min, and the lifting height of the components is set to 12 m. The time to connect a component with the crane is 4 minutes, and the time cost per relocation is 5 minutes. The number of functional node cycles  $N$  in the simulation model is the number of components hoisted during each time period. According to the construction speed,  $N$  of the eight periods is 9, 8, 9, 8, 9, 8, 9, and 8, respectively. The GA-simulation method was used to solve the model. The population size was set as 1000, and the

TABLE 2: Optimized PC component transportation plan.

Date	Factory	Type (quantity)						
Day 1	I	pcb-12 (1)	pcb-22 (1)	pcb-23 (1)	pcb-24 (2)	pcb-25 (1)	pcb-26 (2)	pcb-33 (1)
		pcb-27 (2)	pcb-28 (1)					
		pcb-8 (2)	pcb-9 (2)	pcb-10 (2)	pcb-11 (2)	pcb-12 (2)	pcb-20 (2)	pcb-41 (2)
	II	pcb-29 (2)	pcb-30 (2)	pcb-31 (2)	pcb-32 (2)	pcb-33 (2)	pcb-34 (1)	pcb-42 (1)
		pcb-35 (1)	pcb-36 (2)	pcb-37 (1)	pcb-38 (1)	pcb-39 (2)	pcb-40 (1)	pcb-19 (1)
		III						
Day 2	I	pcb-1 (1)	pcb-2 (1)	pcb-3 (2)	pcb-4 (1)	pcb-5 (2)	pcb-6 (2)	pcb-7 (1)
		pcb-32 (1)	pcb-33 (1)					
		pcb-8 (1)	pcb-9 (1)	pcb-10 (1)	pcb-11 (1)	pcb-16 (1)	pcb-12 (2)	pcb-13 (2)
	II	pcb-14 (2)	pcb-15 (2)	pcb-16 (2)	pcb-17 (2)	pcb-18 (2)	pcb-20 (1)	pcb-21 (2)
		pcb-30 (1)	pcb-31 (1)	pcb-41 (1)				
		III						

TABLE 3: PC component arrival sequence.

Period	Type (quantity)						
1	pcb-12 (1)	pcb-22 (1)	pcb-23 (1)	pcb-24 (2)	pcb-25 (1)	pcb-26 (2)	pcb-27 (2)
	pcb-28 (1)	pcb-33 (1)					
2	pcb-8 (2)	pcb-9 (2)	pcb-10 (2)	pcb-11 (2)	pcb-12 (2)		
3	pcb-20 (2)	pcb-29 (1)	pcb-30 (1)	pcb-31 (1)	pcb-32 (2)	pcb-33 (2)	
4	pcb-34 (1)	pcb-35 (1)	pcb-36 (2)	pcb-37 (1)	pcb-38 (1)	pcb-39 (2)	pcb-40 (1)
	pcb-41 (2)	pcb-42 (1)					
5	pcb-1 (1)	pcb-2 (1)	pcb-3 (2)	pcb-4 (1)	pcb-5 (1)	pcb-6 (2)	pcb-7 (1)
6	pcb-12 (2)	pcb-13 (1)	pcb-14 (1)	pcb-15 (2)	pcb-16 (1)	pcb-18 (2)	
7	pcb-17 (1)	pcb-19 (1)	pcb-21 (1)	pcb-29 (1)	pcb-30 (1)	pcb-31 (1)	pcb-33 (2)
8	pcb-2 (1)	pcb-5 (1)	pcb-6 (1)	pcb-15 (1)	pcb-18 (1)		

number of iterations was 2000. Two parameters of the adaptive crossover rate  $k_1$  and  $k_2$  were 0.75 and 0.8, respectively, and the mutation rate was 0.1. In the simulation model, the two principles are separately used to calculate on-site transportation time. Figure 11 shows the convergence curves of the two principles.

In terms of minimum relocation times, the fitness value of the optimal solution is 2.094. The number of relocation times in the optimization period (2 days) is 8. The horizontal transportation distance is 1247 meters, and the on-site transportation time is 478 minutes. In terms of minimum distance, the fitness value of the optimal solution is 2.017. The number of relocation times is 12. The horizontal transportation distance is 1229 meters, and the transportation time is 496 minutes. The results demonstrate that the optimal solution obtained by the principle of minimum relocation time has a larger fitness value and a shorter on-site transportation time.

In the case study, the difference of horizontal transportation distance of each storage zone was relatively small, and the tower crane had a relatively high transportation speed. Therefore, the impact of difference between the two principles on on-site transportation time was no more than 1 minute on each component. Consequently, the principle of minimum relocation time was more applicable in this case. Figure 12 shows the storage state of period 1 optimized by the principle of minimum relocation time. The storage position of each component can be obtained by subtracting the initial storage state from the state after storage in period 1, as is in the table "Components to be stored" of Figure 12.

The number of layers was counted from top to bottom. The components in a darker colour were already stacked before optimization, while the components in a lighter colour were to be stacked after optimization.

(2) *Result Simulation.* The state after storage in each time period can be obtained according to the optimal solution. The storage positions of PC components in period  $k$  determine the position where a component should be hoisted from during period  $k$ . Therefore, the simulation model was called again to calculate the position and transportation time of each component in period  $k$ . The results of this simulation operation can be used to direct the component hoisting in construction. As an example, Table 4 shows the position and on-site transportation time of each component during period 3.

4.3. *Discussion.* In order to evaluate the effectiveness of the dynamic storage optimization model, a control group model which does not consider the real-time transportation tracking information was developed, and the corresponding on-site transportation time was calculated. In the control group model, PC components which were on the way to the construction site or planned to be transported were not considered. The optimization time period  $T$  of the control group model was 2 hours. In order to keep the optimization time  $T$  of the control group model consistent with that of the original model, the storage of PC components in 8 periods was optimized separately, by assuming that the actual arrival

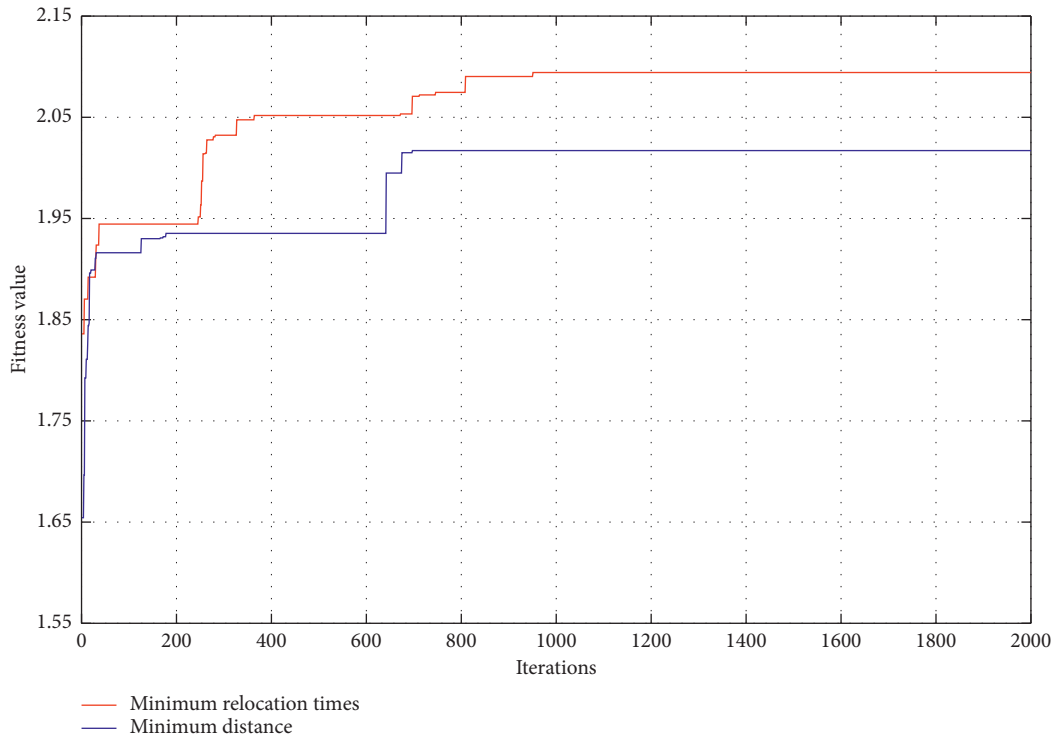


FIGURE 11: GA-simulation convergence curves.

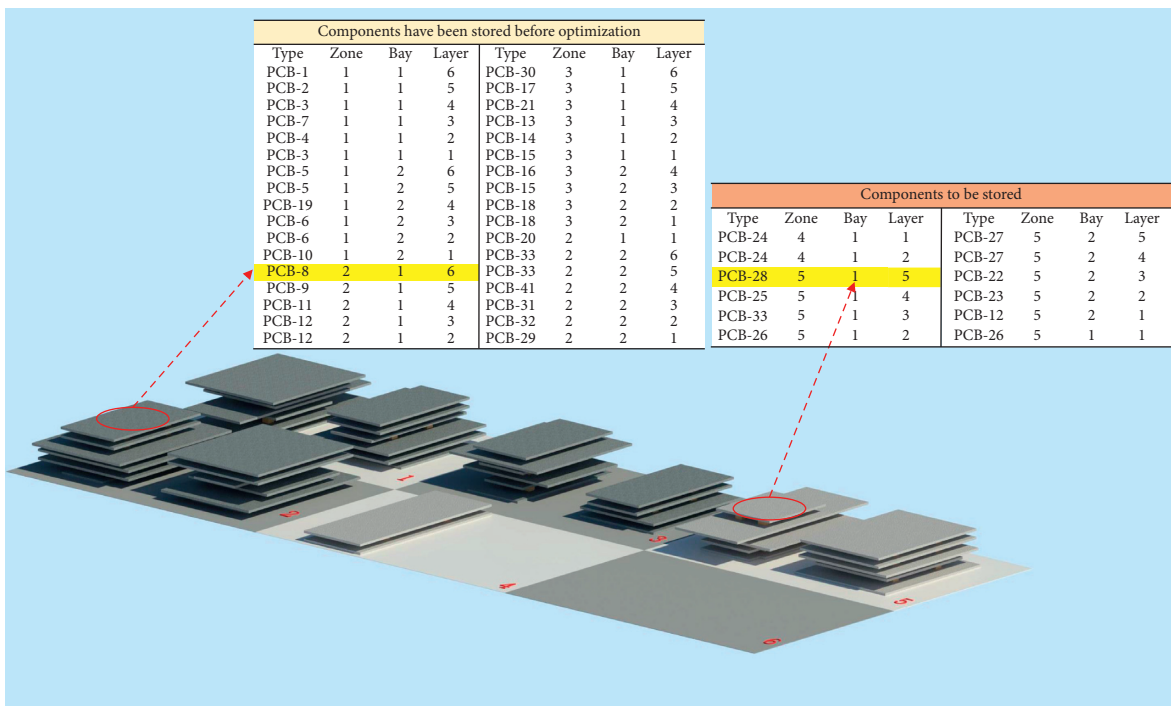


FIGURE 12: BIM of the storage yard after optimization.

time was the same as the results predicted through the transportation tracking. The simulation principle in the control group model was minimum relocation times. The on-site transportation time, the horizontal transportation distance, and the number of relocation times in each period

were obtained. Figure 13 shows the comparison of the results of the control group model and the original model.

When the transportation tracking is not adopted (e.g., the control group model), the number of relocation times was 46 and horizontal transportation distance was 1275.6 m.

TABLE 4: Position and on-site transportation time in the third period.

Hoisting sequence	Type	Hoisting location			On-site transportation time (minutes)	Relocation time
		Zone	Bay	Layer		
1	pcb-20	1	1	2	6.13	0
2	pcb-33	2	2	1	6.29	0
3	pcb-33	2	2	2	6.29	0
4	pcb-41	2	2	3	6.29	0
5	pcb-31	2	2	4	6.29	0
6	pcb-32	1	2	3	6.13	0
7	pcb-29	2	2	6	11.29	1
8	pcb-30	3	2	1	6.53	0
9	pcb-17	3	1	2	6.53	0
Total					61.77	1

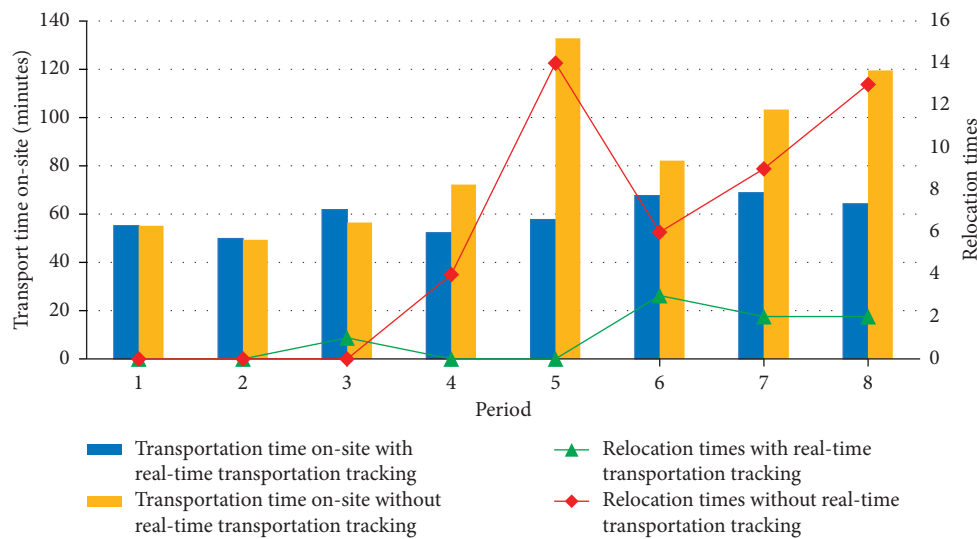


FIGURE 13: Comparison of the results of the control group model and the original model.

The total on-site transportation time was 670.9 minutes. Compared with the original model, the number of relocation times increased by 35 times and the transportation distance increased by 61 m. At the same time, the on-site transportation time increased by 181 minutes, which accounts for about 37% of the total transportation time on-site. The above comparison indicates that the storage optimization based on transportation tracking can effectively reduce the number of relocation times and the on-site transportation time.

As shown in Figure 13, the differences of the number of relocation times and on-site transportation time between the two models are not significant until the later periods of the simulation. In period 5, the on-site transportation time even exceeds the duration of a period (i.e., 120 minutes), which means that too many times of relocation of PC components lead to delay in construction. This is because the components hoisted in the earlier periods had been initially stored in the storage yard before optimization. Nevertheless, the components arriving during optimization periods would be used in subsequent periods. Without transportation tracking to obtain the real-time information of the components' arrival, the control group model ignores the impact of oncoming

components, resulting in a significant increase of relocation times and the on-site transportation time in later periods.

In the case study, the storage yard is small, while the quantity of the component types is relatively huge. Therefore, even though the transportation tracking information has been considered, there still exist relocations in the later periods of the original model. However, compared with the situation where the transportation tracking information is not considered, the number of relocation times is reduced considerably.

## 5. Conclusions

Given the uncertainty of the construction schedule and transportation condition, this study developed the real-time optimization models for the transportation plan and storage layout of PC components based on real-time scheduling and material position tracking. A 4D BIM was adopted to retrieve the real-time schedule. A systematic framework was developed to enable the whole-process tracking of PC components. In order to solve the storage layout optimization model, a CYCLONE simulation model was developed



to simulate the process of component storing and hoisting, and genetic algorithms were used to optimize the on-site transportation time and the relocation times. A case study was implemented in a project located in Z Province in China. The results demonstrate the effectiveness of the proposed models from the following three aspects:

- (1) Compared with the situation without transportation tracking, the results obtained by the storage optimization model can effectively reduce the number of relocation times and on-site transportation time in the PC component construction.
- (2) Using the CYCLONE simulation model for the PC component storing and hoisting, the location and on-site transportation time of each component can be obtained.
- (3) When the storage space is limited and the PC components are in a large quantity, the storage optimization model can make rational use of the storage yard and improve the efficiency on hoisting PC components. Through the real-time tracking system, the whole-process tracking and systematic management of PC components were realized, which can provide the information from leaving factory, transportation, storage on-site, to hoisting and construction.

Further research is needed to address the following limitation: In the proposed models, the transportation time on-site is calculated by considering the linear distance from the storage position to the tower crane position instead of the specific storage position to the installation position, which is not accurate enough. In addition, the installation time of a component is also ignored. In the future study, the BIM can be used to calculate the transportation time of PC components from the yard to the specific installation position, and the coordinated operation of multiple tower cranes needs to be studied to establish a more accurate simulation model to analyze the on-site transportation time.

## Data Availability

The data used to support the findings of this study are available from the corresponding author upon request.

## Conflicts of Interest

The authors declare that there are no conflicts of interest regarding the publication of this paper.

## Acknowledgments

This research was supported by the National Key Research and Development Program of China (No. 2018YFC0406903) and the Innovative Research Groups of the National Natural Science Foundation of China (No. 51621092).

## References

- [1] Z. Xu, S. Wang, and E. Wang, "Integration of BIM and energy consumption modelling for manufacturing prefabricated components: a case study in China," *Advances in Civil Engineering*, vol. 2019, Article ID 1609523, 18 pages, 2019.
- [2] G. Polat, "Factors affecting the use of precast concrete systems in the United States," *Journal of Construction Engineering and Management*, vol. 134, no. 3, pp. 169–178, 2008.
- [3] G. Wu, R. Yang, L. Li et al., "Factors influencing the application of prefabricated construction in China: from perspectives of technology promotion and cleaner production," *Journal of Cleaner Production*, vol. 219, pp. 753–762, 2019.
- [4] C. Z. Li, J. Hong, C. Fan, X. Xu, and G. Q. Shen, "Schedule delay analysis of prefabricated housing production: a hybrid dynamic approach," *Journal of Cleaner Production*, vol. 195, pp. 1533–1545, 2018.
- [5] Y. Fang and S. T. Ng, "Genetic algorithm for determining the construction logistics of precast components," *Engineering, Construction and Architectural Management*, vol. 26, no. 10, pp. 2289–2306, 2019.
- [6] C. Cheng, K. Shen, X. Li, and Z. Zhang, "Major barriers to different kinds of prefabricated public housing in China: the developers' perspective," in *Proceedings of the 2017 International Conference on Construction and Real Estate Management (ICCREM)*, pp. 79–88, Guangzhou, China, November 2017.
- [7] G. Xu, M. Li, L. Luo, C.-H. Chen, and G. Q. Huang, "Cloud-based fleet management for prefabrication transportation," *Enterprise Information Systems*, vol. 13, no. 1, pp. 87–106, 2019.
- [8] Y. Zhai, R. Y. Zhong, Z. Li, and G. Huang, "Production lead-time hedging and coordination in prefabricated construction supply chain management," *International Journal of Production Research*, vol. 55, no. 14, pp. 3984–4002, 2017.
- [9] C. Chang, F. Wu, and D. Liu, "Optimization model of load and transportation for prefabricated construction components," in *Proceedings of the 2016 International Forum on Energy, Environment and Sustainable Development (IFEESD)*, pp. 1145–1148, Shenzhen, China, May 2016.
- [10] X. Tang, P. Xu, and S. Cui, "Applying the bi-level programming model based on time satisfaction to optimize transportation scheduling of prefabricated components," in *Proceedings of the 2019 8th International Conference on Industrial Technology and Management (ICITM)*, pp. 280–284, Cambridge, UK, March 2019.
- [11] P. Alanjari, S. Razavialavi, and S. Abourizk, "A simulation-based approach for material yard laydown planning," *Automation in Construction*, vol. 40, no. 3, pp. 1–8, 2014.
- [12] S. S. Kumar and J. C. P. Cheng, "A BIM-based automated site layout planning framework for congested construction sites," *Automation in Construction*, vol. 59, pp. 24–37, 2015.
- [13] H. Said and K. El-Rayes, "Optimal utilization of interior building spaces for material procurement and storage in congested construction sites," *Automation in Construction*, vol. 31, no. 3, pp. 292–306, 2013.
- [14] H. Said and K. El-Rayes, "Automated multi-objective construction logistics optimization system," *Automation in Construction*, vol. 43, pp. 110–122, 2014.
- [15] I. N. Papadaki and A. P. Chassiakos, "Multi-objective construction site layout planning using genetic algorithms," *Procedia Engineering*, vol. 164, pp. 20–27, 2016.
- [16] K.-C. Lam, X. Ning, and M. C.-K. Lam, "Conjoining MMAS to GA to solve construction site layout planning problem," *Journal of Construction Engineering and Management*, vol. 135, no. 10, pp. 1049–1057, 2009.
- [17] T.-H. Shin, S. Chin, S.-W. Yoon, and S.-W. Kwon, "A service-oriented integrated information framework for RFID/WSN-

- based intelligent construction supply chain management,” *Automation in Construction*, vol. 20, no. 6, pp. 706–715, 2011.
- [18] J. Song, C. T. Haas, C. Caldas, E. Ergen, and B. Akinci, “Automating the task of tracking the delivery and receipt of fabricated pipe spools in industrial projects,” *Automation in Construction*, vol. 15, no. 2, pp. 166–177, 2006.
- [19] S. Y. L. Yin, H. P. Tserng, J. C. Wang, and S. C. Tsai, “Developing a precast production management system using RFID technology,” *Automation in Construction*, vol. 18, no. 5, pp. 677–691, 2009.
- [20] V. Hinkka and J. Tätilä, “RFID tracking implementation model for the technical trade and construction supply chains,” *Automation in Construction*, vol. 35, pp. 405–414, 2013.
- [21] C. Z. Li, R. Y. Zhong, F. Xue et al., “Integrating RFID and BIM technologies for mitigating risks and improving schedule performance of prefabricated house construction,” *Journal of Cleaner Production*, vol. 165, pp. 1048–1062, 2017.
- [22] J. Majrouhi Sardroud, “Influence of RFID technology on automated management of construction materials and components,” *Scientia Iranica*, vol. 19, no. 3, pp. 381–392, 2012.
- [23] R. Y. Zhong, Y. Peng, F. Xue et al., “Prefabricated construction enabled by the internet-of-things,” *Automation in Construction*, vol. 76, pp. 59–70, 2017.
- [24] Y. Fang, Y. K. Cho, S. Zhang, and E. Perez, “Case study of BIM and cloud-enabled real-time RFID indoor localization for construction management applications,” *Journal of Construction Engineering and Management*, vol. 142, no. 7, Article ID 05016003, 2016.
- [25] C. Z. Li, F. Xue, X. Li, J. Hong, and G. Q. Shen, “An internet of things-enabled BIM platform for on-site assembly services in prefabricated construction,” *Automation in Construction*, vol. 89, pp. 146–161, 2018.
- [26] E. Ergen, B. Akinci, and R. Sacks, “Tracking and locating components in a precast storage yard utilizing radio frequency identification technology and GPS,” *Automation in Construction*, vol. 16, no. 3, pp. 354–367, 2007.
- [27] R. Chavada, N. Dawood, and M. Kassem, “Construction workspace management: the development and application of a novel nD planning approach and tool,” *Electronic Journal of Information Technology in Construction*, vol. 17, pp. 213–236, 2012.
- [28] R. Bortolini, J. S. Shigaki, and C. T. Formoso, “Site logistics planning and control using 4D modeling: a study in a lean car factory building site,” in *Proceedings of the 2015 Conference of the International Group for Lean Construction*, Perth, Australia, July 2015.
- [29] R. Bortolini, C. T. Formoso, and D. D. Viana, “Site logistics planning and control for engineer-to-order prefabricated building systems using BIM 4D modeling,” *Automation in Construction*, vol. 98, pp. 248–264, 2019.
- [30] K. Shih, C. Huang, S. Liu et al., “Study on the storage and transportation optimization of pre-fabrication factory,” in *Proceedings of the 2005 22nd International Symposium on Automation and Robotics in Construction*, Ferrara, Italy, September 2005.
- [31] N. Dawood and R. Marasini, “Visualisation of a stockyard layout simulator “SimStock”: a case study in precast concrete products industry,” in *Proceedings of the 7th International Conference on Virtual Systems and Multimedia*, pp. 726–737, IEEE, Berkeley, CA, USA, October 2001.
- [32] D. Liu, P. Xuan, S. Li, and P. Huang, “Schedule risk analysis for TBM tunneling based on adaptive cyclone simulation in a geologic uncertainty-aware context,” *Journal of Computing in Civil Engineering*, vol. 29, no. 6, Article ID 04014103, 2015.
- [33] D. Zhong, J. Li, H. Zhu, and L. Song, “Geographic information system-based visual simulation methodology and its application in concrete dam construction processes,” *Journal of Construction Engineering and Management*, vol. 130, no. 5, pp. 742–750, 2004.